Supporting Information

Single-molecule white organic light-emitting diodes based on dual-conformation diindolophenthiazine derivatives

Juan Rui[a], Junrong Pu[a], Zijian Chen[b], Hao Tang[a], Lingyun Wang[a], Shi-Jian Su *[b] and Derong Cao*[a]

[a] State Key Laboratory of Luminescent Materials and Devices, and School of Chemistry and Chemical Engineering, South China University of Technology, Wushan Road 381, Guangzhou 510641, China.

[b] State Key Laboratory of Luminescent Materials and Devices, and Guangdong Basic Research Center of Excellence for Energy & Information Polymer Materials, South China University of Technology, Wushan Road 381, Guangzhou 510641, China.

Contents

1. Materials, characterizations and methods

2. Scheme, Figures and Tables

3. Reference

1. Materials, characterizations and methods

Experimental materials and reagents

4-Bromo-benzophenon, tri-tert-butyl, tris(dibenzylideneacetone)dipalladium, phenothiazine, 1-bromonitrobenzene, triphenylphosphine were purchased from Adamas Reagent Company in China. Potassium phosphate and potassium hydroxide were purchased from Shanghai Aladdin Pharmaceutical Company. Iodomethane, N-bromobutyramide, bis(diboronato)diboron were purchased from Shanghai Bide Pharmaceutical Technology Co., Ltd. Sodium tert-butoxide, tetrakis(triphenylphosphine)palladium and 1,1'-bis (diphenylphosphino)ferrocene (dppf) were purchased from Beijing Bailing Wei Science and Technology Co., Ltd. THF, toluene, 1-4-dioxane, etc. were all dried and deoxygenated by sodium metal particle. Ultra-dry *o*-dichlorobenzene was from Shanghai McLean Biochemical Technology Co., Ltd. Other reagents and solvents were from domestic reagent companies. The silica gel of column chromatography was 200-300 mesh and 300-400 mesh.

Structural Characterization Instruments for New Compounds

The new compounds described in this chapter have been characterized by ^{1}H NMR,^{13}C NMR as well as HRMS (MALDI-TOF) and melting point instrumentation to determine their structures. ^{1}H NMR,^{13}C NMR were done on Bruker AM 400 MHz and Bruker AM 500 MHz spectrometer, the deuterated reagents used for the tests were $CDCl_3$, and tetramethylsilane as internal standard. HRMS (MALDI-TOF) was conducted on a Waters SYNAPT G2-Si mass spectrometer. The melting point was determined by a WRS-2 microcomputer melting point apparatus from Shanghai Yidian Physical and Optical Instrument Co., Ltd.

Theoretical Calculation

The electron density distribution of frontier molecular orbitals (FOMs) were visualized with Gauss view 5.0. All ground state geometries were optimized in B3LYP-D3(BJ)/6-31G* level in the gas phase by density functional theory (DFT). The S_1 geometries were optimized in B3LYP-D3(BJ)/6-31G* level in the gas phase according to the time-dependence density functional theory (TD-DFT). Further frequency analyses were calculated in optimized geometries to accurately find the local minima. Based on the optimized geometries, excited state properties were subsequently investigated using TD-DFT. Based on the optimized geometries, excited state properties were subsequently investigated using TD-DFT in the B3LYP-D3(BJ)/6-311G* level.

Electrochemical Characterization

The oxidation and reduction potential were determined by cyclic voltammetry using 0.1 M tetrabutylammonium hexafluorophosphate ($TBAPF_6$) in CH_2Cl_2 as a supporting A 3-electrode cell comprising

Ag/AgCl, a platinum mesh and ITO as the reference, counter, and working electrodes, respectively. All potentials were recorded versus Ag/AgCl (saturated) as a reference electrode. Oxidation of the ferrocene/ferrocenium (Fc/Fc^+) redox couple in CH_2Cl_2/TBAPF6 occurs at E_{ox} = +4.8 V. HOMO and LUMO levels were conducted from the oxidation and reduction half-wave potential with the formula: $E_{HOMO/LUMO} = -(E_{oxi.\ v.\ s.\ Fc+/Fc} + 4.8)$ (eV).

Photophysical Characterization

Absorption spectra were studied using a UV-vis spectrophotometer (HITACHI U-3900H). Photoluminescence (PL) spectra and phosphorescence spectra were performed using a HITACHI F-4600 spectrophotometer. The transient fluorescence decay characteristics were measured using an Edinburgh Instruments FLS980 spectrometer. The transient fluorescence decay characteristics were measured using an Edinburgh Instruments FLS980 spectrometer. The temperature dependence experiment is conducted under the temperature dependence experiment is conducted under low temperature refrigeration system from Advanced Research Systems Company. The absolute fluorescence quantum yields of the solid films are measured.

OLED Fabrication and Characterization

After the cleaned indium tin oxide (ITO, 95 nm) substrates were treated with O_2 plasma for 120 s, PEDOT: PSS (4083, Xian Polymer Light Technology Co., Ltd.) was spin-coated onto the treated ITO at 3000 rpm for 30 s to form 35 nm hole injection layer, then backed at 80 ℃ for 15 min. Meanwhile, the preheated (@ 50 ℃, 12 h) luminescent layer solutions (hosts and CBP: 10 mg/mL, in chlorobenzene) are cooled down to room temperature. Then, by dropping the liquid (50 μL) onto the center of ITO substrate, immediately, a 30 nm EML layer was spin-coated at 3000 rpm for 30 s for reducing the intermixing of two adjacent layers. Finally, the EML layer was annealed at 80 ℃ for 15 min and then immediately transferred to the evaporation chamber for avoiding solvents erosion. The electron transporting layer TmPyPB as well as cathode (i.e., CsF and Al) were then successively deposited under the vacuum below 1×10^{-4} Pa (active area:10 mm^2), the thickness of various transporting materials was monitored by a quartz crystal thickness monitor (SQC-310, Inficon). The doping concentration of vacuum evaporated EMLs were controlled by their deposited rate, the rest processing routes remain unchanged. Before the characterization, all the devices were encapsulated with a UV-cured epoxy resin. The electroluminescent characteristics of devices were collected by XPQY-EQE-350-1100 (Guangzhou Xi Pu Optoelectronics Technology Co., Ltd.) and powered by Keithley 2400, equipped with an integrated sphere (GPS-4P-SL, Labsphere) and a photodetector array (S7031-1006, Hamamatsu Photonics). The operation lifetimes of devices were recorded by a well-established measurement system (Crysco Test).

The transient EL decay profiles are recorded by an Edinburgh FL980 fluorescence spectrophotometer and driven by a digital oscilloscope (Tektronix, AFG3152C). The J-V characteristics of the hole-only and electron-only devices were measured by a Photo Research PR745 instrument under dark environment, equipped with a Keithley 2450.

2. Scheme, Figures and Tables

2.1. Synthesis and characterization of target compounds and intermediates.

Synthesis of *(4-(3,7-bis(4,4,5,5-tetramethyl-1,3,2-dioxaborolan-2-yl)-10H-phenothiazin-10-yl)phenyl)(phenyl)methanone* (3)

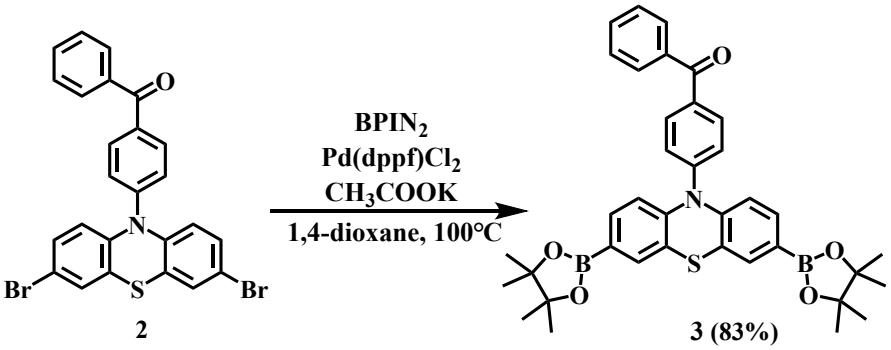

Compound **2** (2.11 mmol, 1.13 g), bis(pinacolato)diboron (6.37 mmol, 1.61 g), potassium acetate (7.96 mmol, 0.78 g), Pd(dppf)Cl_2 (0.2 mmol, 150 mg), and 30 ml of dried 1,4-dioxane were added to a 100 ml two-necked bottle. The mixture was stirred at 100 °C for 24 h under N_2 atmosphere. After cooling to room temperature, water was added to quench the reaction. The mixture was then extracted with CH_2Cl_2 three times. The solvent was removed under reduced pressure, and the crude product was purified by silica gel using column chromatography with petroleum ether/ dichloromethane (v/v=5:1) as the eluent. The compound **3** was obtained as a yellow solid in 83% yield (1.105 g). Melting point: 216.7~217.9 °C. ^{1}H NMR (400 MHz, $CDCl_3$) δ 8.00–7.98 (m, 2H), 7.87–7.84 (m, 2H), 7.63–7.59 (m, 1H), 7.53–7.49 (m, 4H), 7.43–7.40 (m, 2H), 7.37 (dd, J = 8.24, 1.4 Hz, 2H), 6.38 (d, J = 8.16 Hz, 2H), 1.31 (s, 24H). ^{13}C NMR (100MHz, $CDCl_3$) δ 195.61, 145.29, 145.07, 137.39, 136.03, 133.72, 133.68, 132.65, 132.63, 130.02, 128.45, 127.60, 123.99, 122.46, 117.44, 83.84, 24.85. HRMS (MALDI–TOF, *m/z*): $[M+H]^+$ calcd for $C_{37}H_{40}B_2NO_5S$, 631.2735; found, 631.2848.

Synthesis of *(4-(3,7-bis(2-nitrophenyl)-10H-phenothiazin-10-yl)phenyl)(phenyl)methanone* (4)

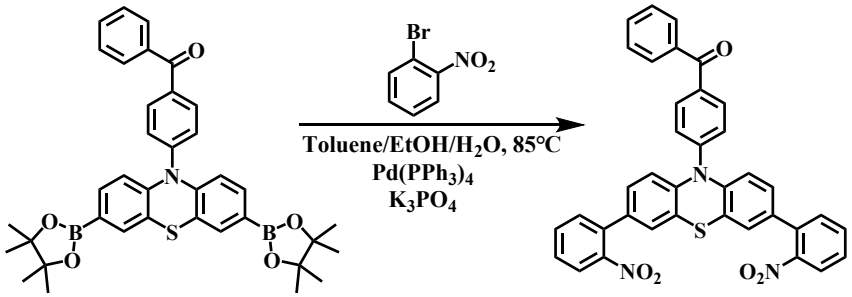

3 4 (80%)

Compound **3** (1.8 mmol, 1.14 g), 1-bromo-2-nitrobenzene (5.41 mmol, 1.09 g), K_3PO_4 (6.60 mmol, 1.40 g), $Pd(PPh_3)_4$ (0.18 mmol, 207 mg), 50 ml of toluene, 10 ml of ethanol, and 5 ml of water were added to a 100-ml two-necked bottle. Then the mixture was stirred for 85 °C for 24 h under N_2 atmosphere. After cooling to room temperature, water was added to quench the reaction. The mixture was then extracted with CH_2Cl_2 three times. The solvent was removed under reduced pressure, and the crude product was purified by silica gel using column chromatography with petroleum ether/ dichloromethane (v/v=5:2) as the eluent. The compound **4** was obtained as a red solid in 80% yield (895 mg). Melting point: 232.4~235.0 °C.^{1}H NMR (500 MHz, $CDCl_3$) δ 8.04–8.02 (m, 2H), 7.88–7.82 (m, 4H), 7.65–7.58 (m, 3H), 7.55–7.45 (m, 6H), 7.40 (dd, *J* = 7.65, 1.00 Hz, 2H), 7.10 (d, *J* = 2.00 Hz, 2H), 6.91 (dd, *J* = 8.45, 2.05 Hz, 2H), 6.50 (d, *J* = 8.45 Hz, 2H). ^{13}C NMR (125 MHz, $CDCl_3$) δ 195.57, 149.05, 145.05, 142.98, 137.35, 136.29, 134.88, 132.90, 132.69, 132.68, 132.42, 131.70, 130.04, 128.47, 128.28, 127.70, 126.85, 126.69, 124.21, 123.34, 118.21. HRMS (MALDI–TOF, *m/z*): $[M+H]^+$ calcd for $C_{37}H_{24}N_3SO_5$, 622.1358; found, 622.1439.

Synthesis of *(4-(9,16-dimethyl-9H-diindolo[2,3-b:2',3'-h]phenothiazin-7(16H)-yl)phenyl)(phenyl)methanone* (BP1)

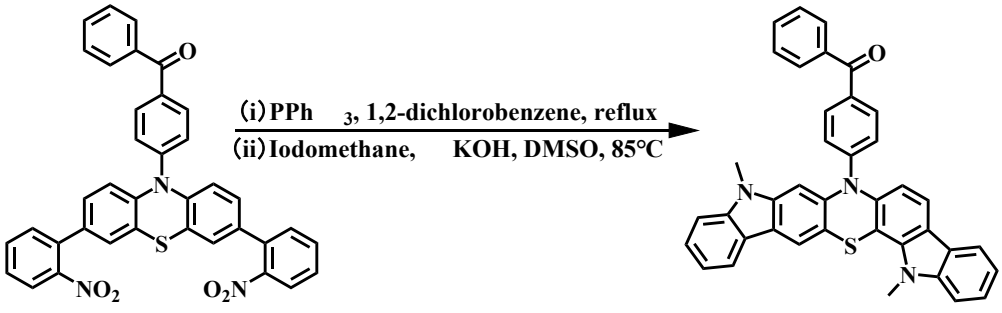

4 BP1 (20%)

(i) Compound **4** (0.97 mmol, 621 mg), PPh_3 (9.7 mmol, 2.54 g) and 20 ml of ultra-dry *o*-dichlorobenzene (*o*-DCB) ware added in a 100 ml two-necked bottle. Nitrogen was introduced and evacuated with vacuum pump for 30 minutes. The mixture stirred and heated to reflux and was continued for 24 h. *o*-DCB was

removed by distillation under reduced pressure after reaction was stopped. The crude product obtained was separated by column chromatography using the eluting agent petroleum ether/ dichloromethane/ ethyl acetate (v/v=12:2:1). The earthy solid obtained was directly put into the next step of the reaction. (ii) The earthy solid obtained from the previous step was added to a 100 ml two-necked bottle. 1-Iodomethane (2.26 mmol, 480 mg), KOH (2.26 mmol, 126 mg), DMSO (40 ml) ware added under nitrogen. After evacuating for 15 minutes by vacuum pump, the reaction mixture was stirred and heated at 85°C for 24 h. After that deionized water (100 mL) was added to the mixture, and the resulting yellow solid was collected by filtration and washed with water (100 mL) three times to give **BP1** as a yellow solid in 20% yield (113 mg). Melting point: 279.9–282.9°C. ^{1}H NMR (400 MHz, $CDCl_3$) δ 8.28 (s, 1H), 8.09– 8.06 (m, 3H), 7.78–7.74 (m, 4H),7.69 (s, 1H), 7.54–7.50 (m, 4H),7.47–7.41 (m, 4H), 7.31–7.28 (m, 2H), 7.13 (d, *J* = 8.80 Hz, 2H), 4.32 (s, 3H), 3.86 (s, 3H). ^{13}C NMR (100 MHz, $CDCl_3$) δ 195.23, 151.19, 142.16, 141.97, 140.88, 140.51, 140.37, 138.97, 138.71, 134.22, 132.29, 131.54, 129.63, 128.70, 128.09, 126.31, 126.12, 125.42, 122.36, 122.15, 121.82, 121.55, 120.40, 120.17, 119.72, 119.65, 119.55, 118.83, 112.99, 111.88, 108.91, 108.74, 108.05, 32.86, 29.40. HRMS (MALDI–TOF, *m/z*): $[M]^+$ calcd for $C_{39}H_{27}N_3OS$, 585.1875; found, 585.1597.

Synthesis of *(4-(14,16-dimethyl-14H-diindolo[3,2-c:2',3'-h]phenothiazin-7(16H)-yl)phenyl)(phenyl)methanone* (BP2)

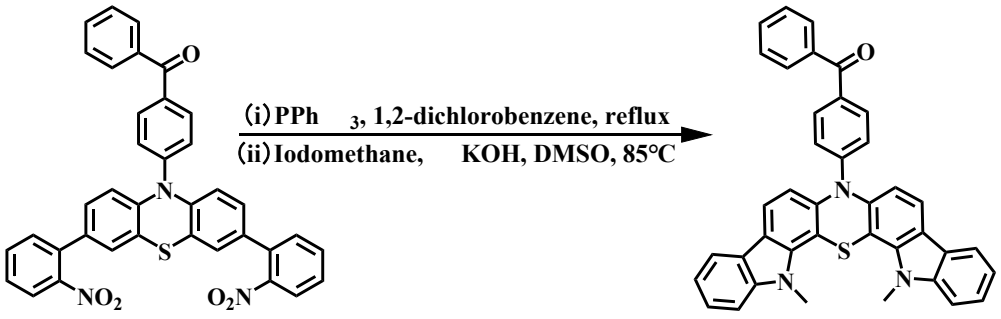

4 **BP2 (5%)**

The synthesis was described with reference to the synthesis of **BP1** above, resulting in a yellow solid in 5% yield. Melting point: 291.5–293.9°C.^{1}H NMR (500 MHz, $CDCl_3$) δ 8.06–8.03 (m, 4H), 7.71–7.67 (m, 4H), 7.49–7.46 (m, 5H), 7.41–7.38 (m, 4H), 7.24 (d, *J* = 6.45 Hz, 2H), 7.04 (d, *J* = 8.90 Hz, 2H), 4.3 (s, 6H). ^{13}C NMR (125 MHz, $CDCl_3$) δ 195.15, 150.98, 142.04, 141.37, 138.94, 138.80, 132.25, 131.44, 129.59, 128.47, 128.05, 126.17, 122.39, 122.22, 120.21, 119.88, 119.59, 119.42, 118.66, 112.44, 108.81, 32.79. HRMS (MALDI–TOF, *m/z*): $[M]^+$ calcd for $C_{39}H_{27}N_3OS$, 585.1875; found, 585.2578.

2.2. Figures

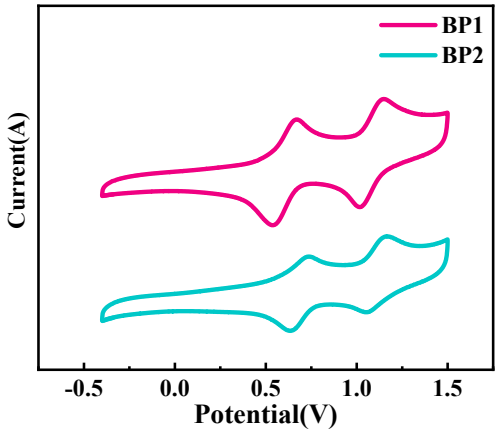

Figure S1. Cyclic voltammograms of **BP1** and **BP2** in DCM solution.

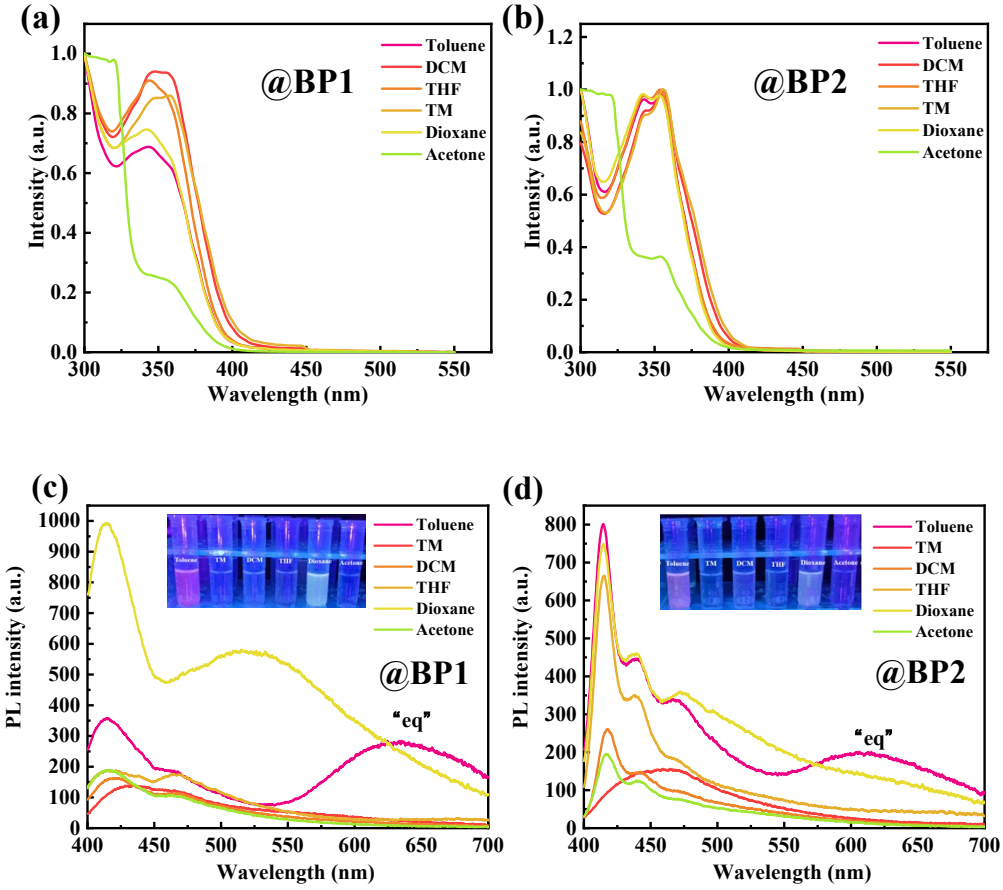

Figure S2. UV–Vis absorption spectra of **BP1** (a) and **BP2** (b) in various solutions (10^{-4} M). PL spectra of **BP1** (c) and **BP2** (d) in various solutions (10^{-4} M). **BP1** exhibits enhanced white fluorescence and dual emissions from "ax" and "eq" conformers in dioxane solution. In **BP2**, the peaks between 400 nm and 470 nm exhibit little redshift in various solutions, showing the characteristics of local excitation. Both compounds exhibit red emission peaks attributed to "eq" conformer in toluene, which indicate a hybrid local excited and charge transfer character in different solutions.

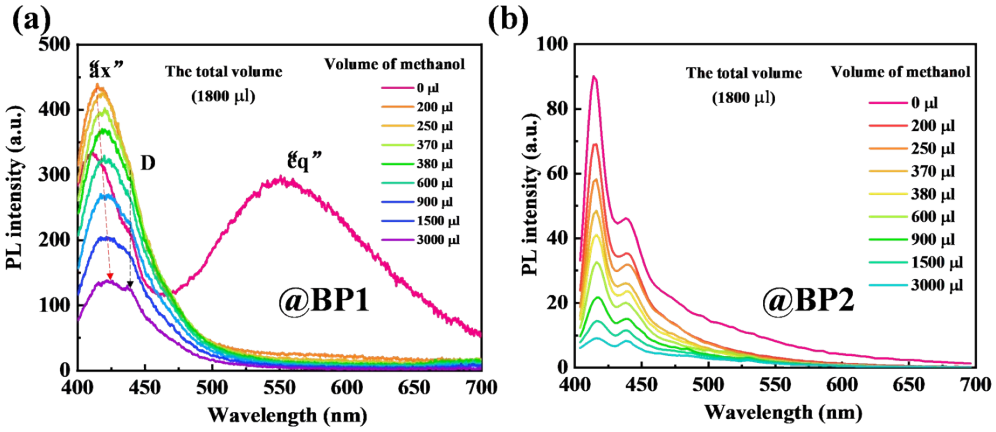

Figure S3. The emission spectra of **BP1** (a) and **BP2** (b) by gradual addition of methanol in THF solution (10^{-4} M).

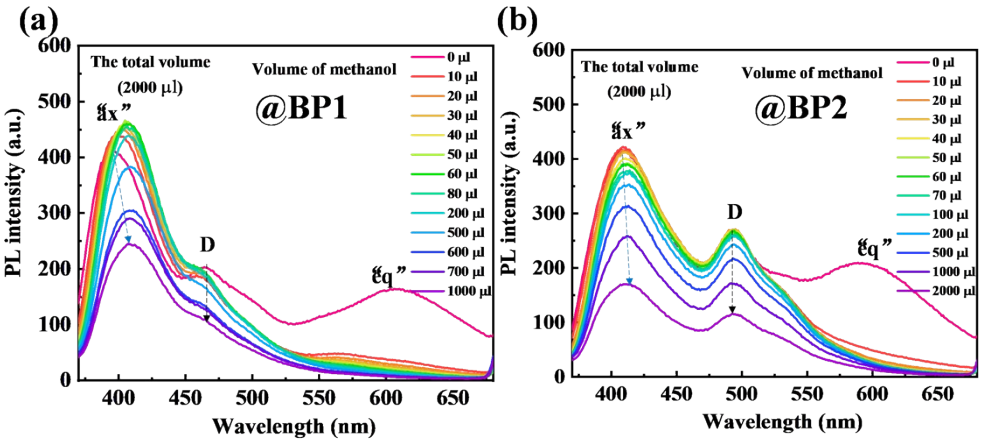

Figure S4. Changes in the emission spectra of **BP1** (a) and **BP2** (b) by gradual addition of methanol in toluene solution (10^{-4} M).

The emission spectra of **BP1** in different solvents (toluene, chloroform, THF, DCM, dioxane, acetone, see Figure 2) are investigated. The emission peak and intensity of the emission at around 630 nm obviously exhibited vastly disappeared as the polarity of the solvent increased, which indicated its stronger CT character. While for the first emission at around 420 nm, its intensity also gradually decreased with the polarity of the solvent increased. This result further proved that wake CT emission comes from ax-conformer, and stronger CT comes from "eq" conformer. Further, the emission spectra of **BP1** in Toluene/CH_3OH and THF/CH_3OH have been measured as shown in Figure S3 and S4, which further prove the CT character of two emissions. We cannot found the emission from "eq" conformer (higher energy emission) in THF/ CH_3OH because of this emission exhibit obvious CT character, which will disappear in stronger polarity solution. This has been proved in our article (Figure S2). On the other hand, we can find that the emission from "ax" conformer (lower energy emission) also exhibit CT character, because of the wavelength redshifted with the increase of volume of methanol. The peak around 480 nm is attributed to the donor which exhibit LE character.[1]

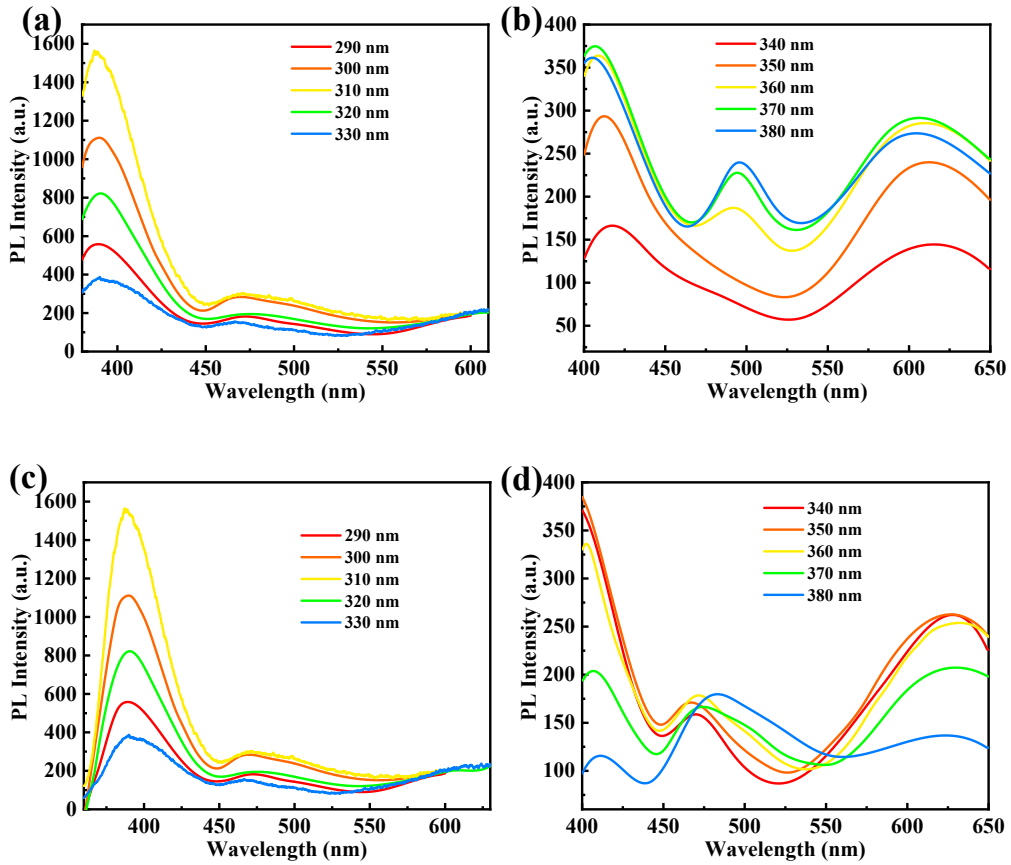

Figure S5. PL spectra of **BP1** in toluene (10^{-4} M) (a)(b) at different excitation wavelengths. PL spectra of **BP2** in toluene (10^{-4} M) (c)(d) at different excitation wavelengths.

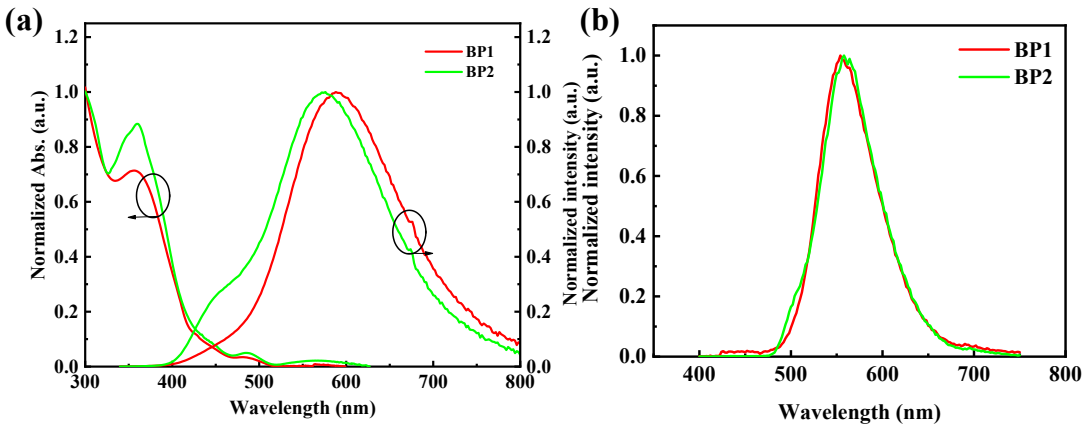

Figure S6. (a) Absorption and PL spectra of **BP1** and **BP2** in neat films at room temperature. (b) Normalized phosphorescence spectra of **BP1** and **BP2** neat films at 77 K with delay lifetime of 20 ms.

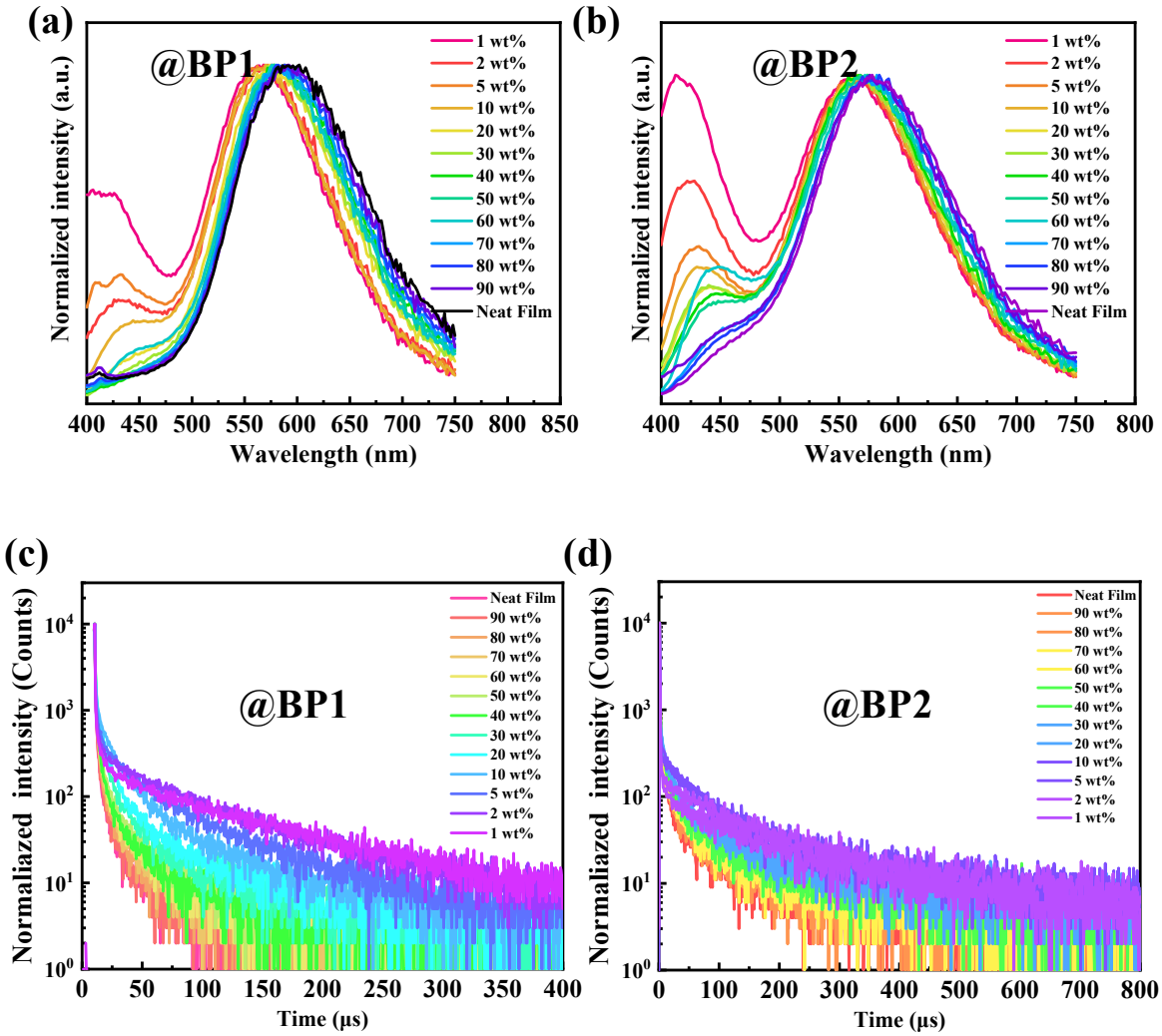

Figure S7. (a) PL spectra of **BP1** neat and doped films. (b) PL spectra of **BP2** neat and doped films. Transient decay characteristics: (c) **BP1** neat and doped films at 580 nm. (d) **BP2** neat and doped films at 574 nm.

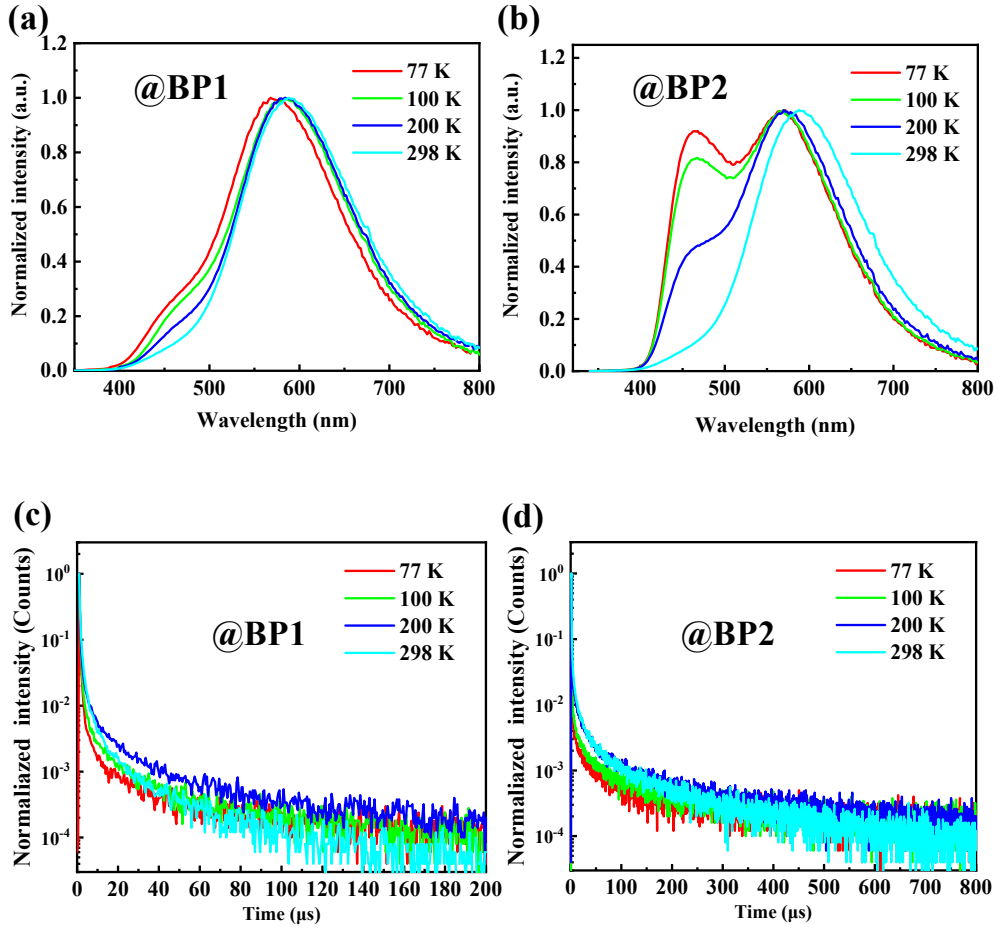

Figure S8. PL spectra of **BP1** (a) and **BP2** (b) at different temperatures (77, 100, 200, and 300 K). Transient decay spectra of **BP1** (c) and **BP2** (d) at different temperatures (77, 100, 200, and 300 K) at 580 nm and 574 nm, respectively.

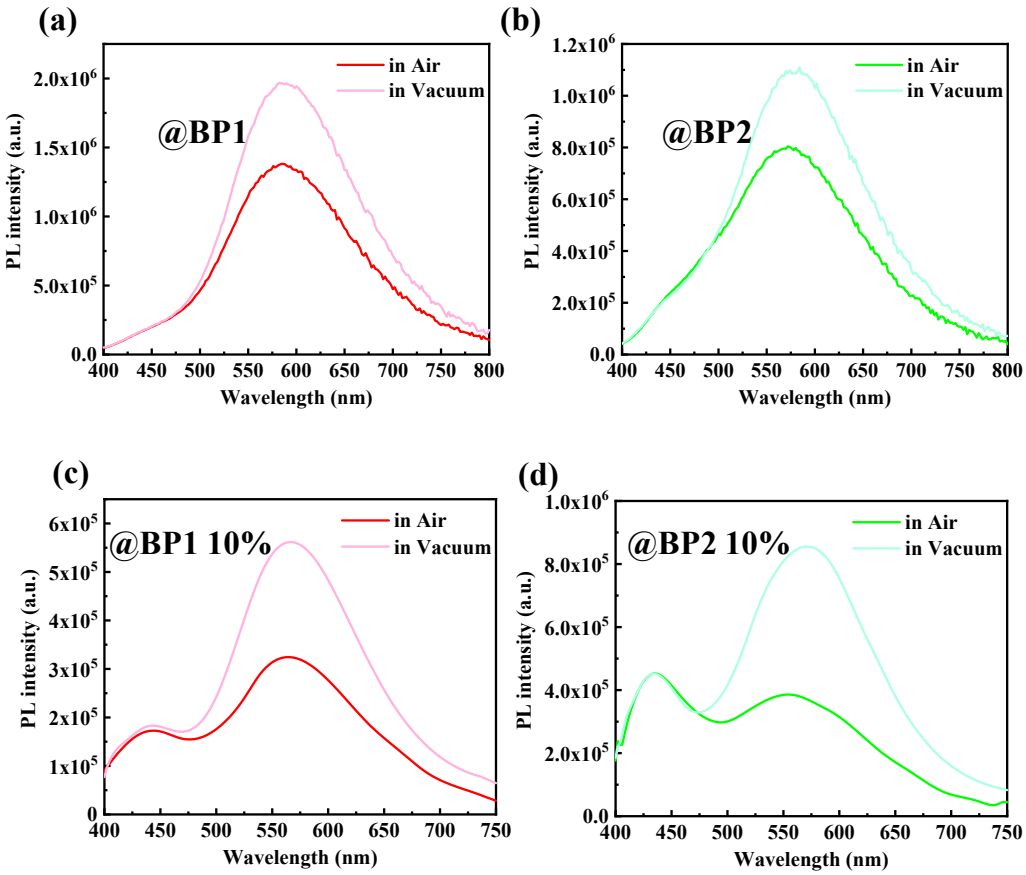

Figure S9. PL spectra of **BP1** (a) and **BP2** (b) neat film in air and vacuum. PL spectra of 10 wt. % **BP1**: CBP film (c) and10 wt. % **BP2**: CBP film (d) in air and vacuum.

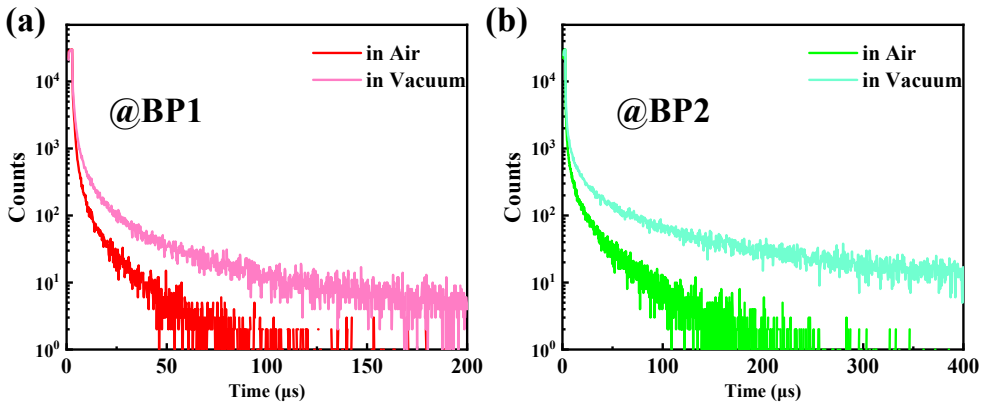

Figure S10. (a) 580 nm transient decay spectrum of **BP1** neat film in air and vacuum. (b) 574 nm transient decay spectrum of **BP2** neat film in air and vacuum.

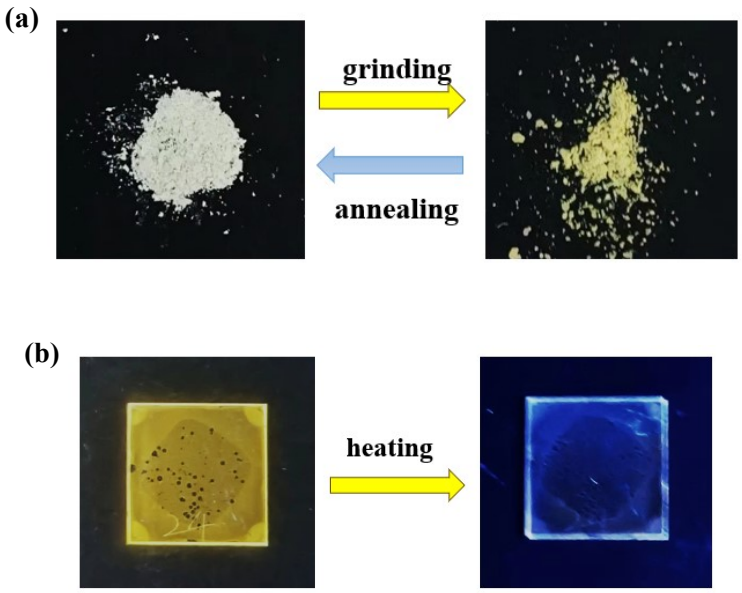

Figure S11. (a) Photographs of **BP1** original crystalline powder before and after grinding taken under daylight. (b) Photographs of **BP1** film taken under 365 nm UV irradiation and after heating at 160℃ for 2h.

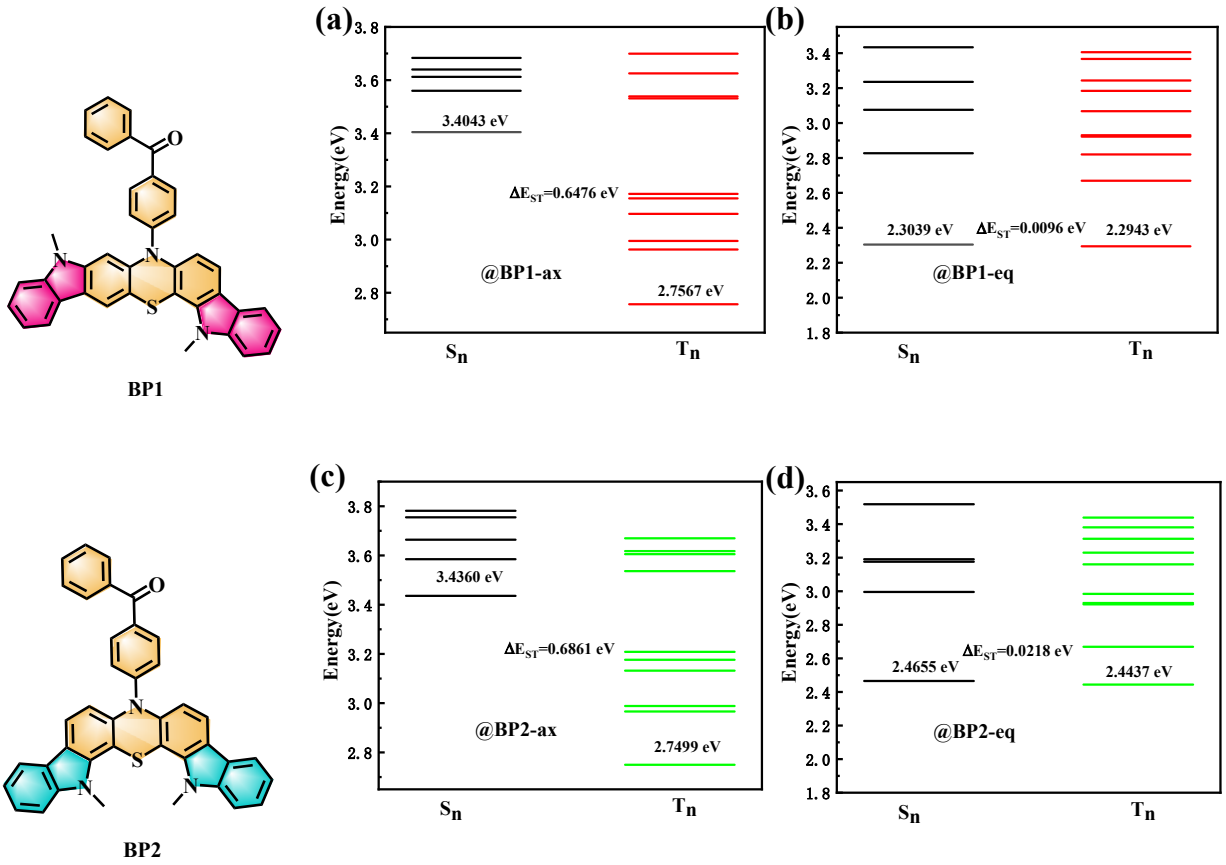

Figure S12. BP1 "ax" (a) "eq" (b) and **BP2** "ax" (c) "eq " (d) Schematic diagrams of the energy levels of the two conformations in the singlet and triplet states.

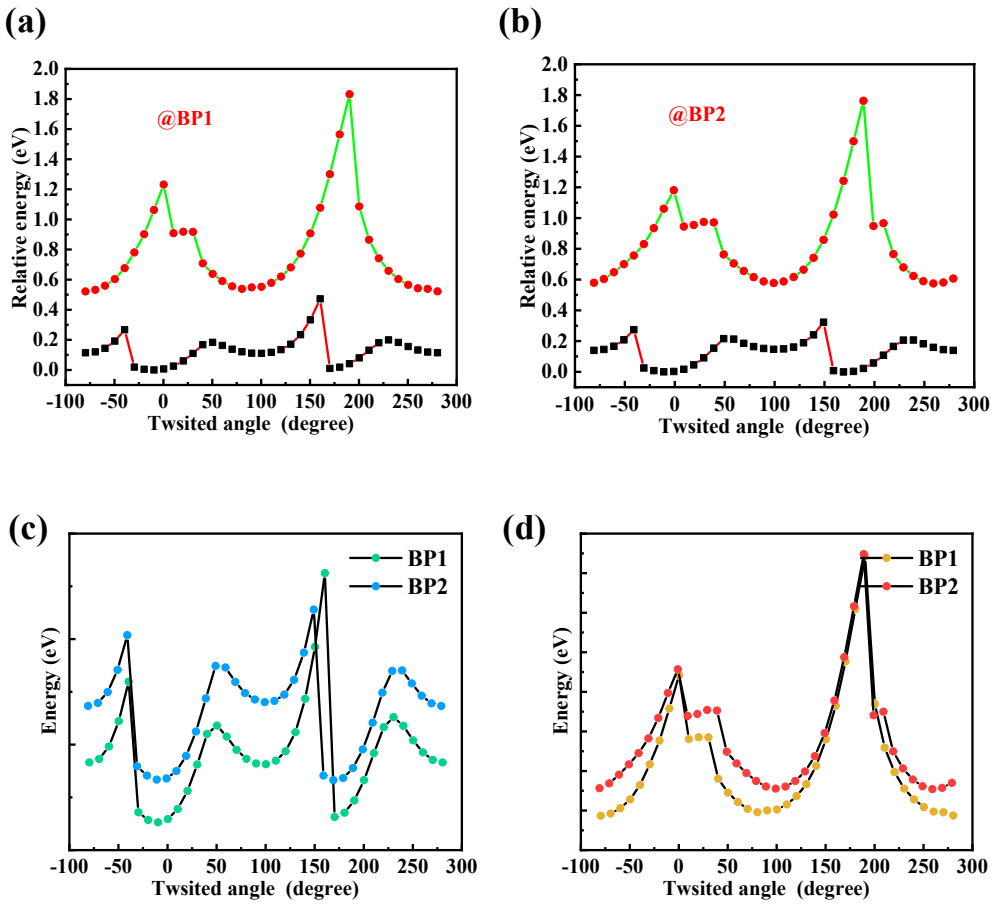

Figure S13. Flexible potential energy surface scans of the ground and excited states **BP1**(a) and **BP2**(b) at different torsion angles. Scans of the flexible potential energy surfaces of the ground (c) and excited (d) states of **BP1-2** at different torsion angles.

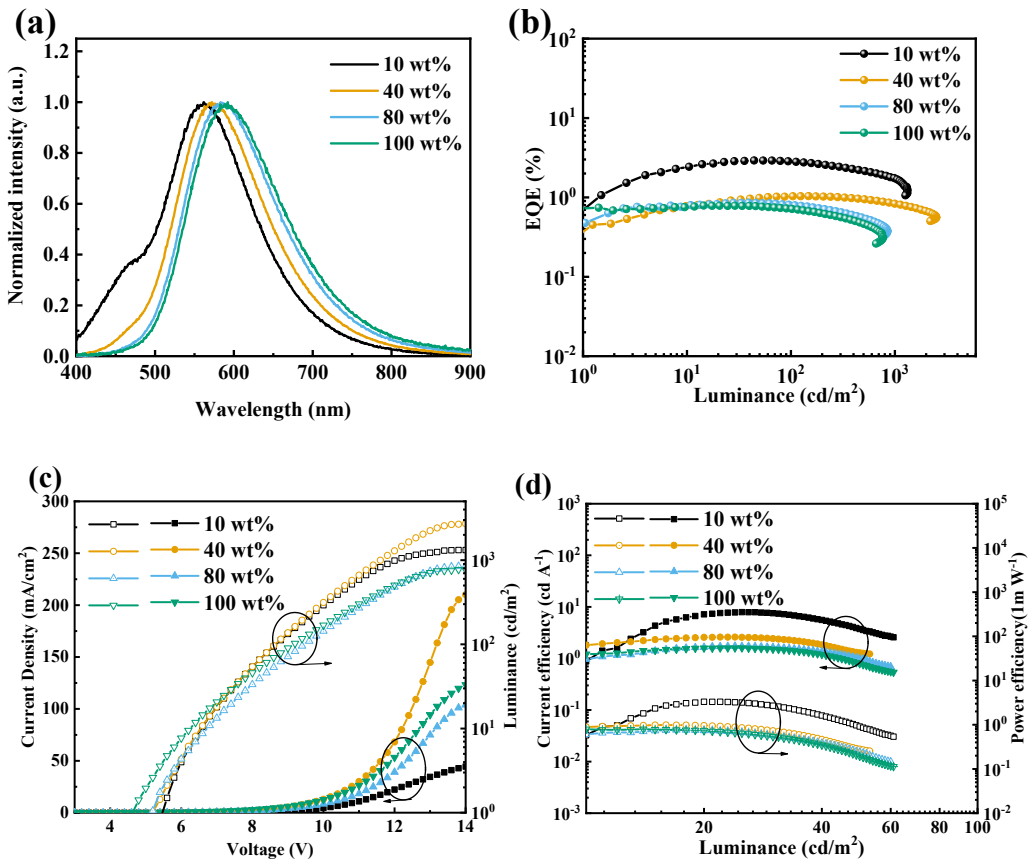

Figure S14. Performance of **BP1**-based OLED with doped different concentration (10%, 40%, 80%, and 100%. (a) EL spectra at 14V. (b) External quantum efficiency (η_{ext}) versus current density plots. (c) Current density and luminance versus voltage (*J-V-L*) characteristics. (d) Current efficiency-luminance-power efficiency.

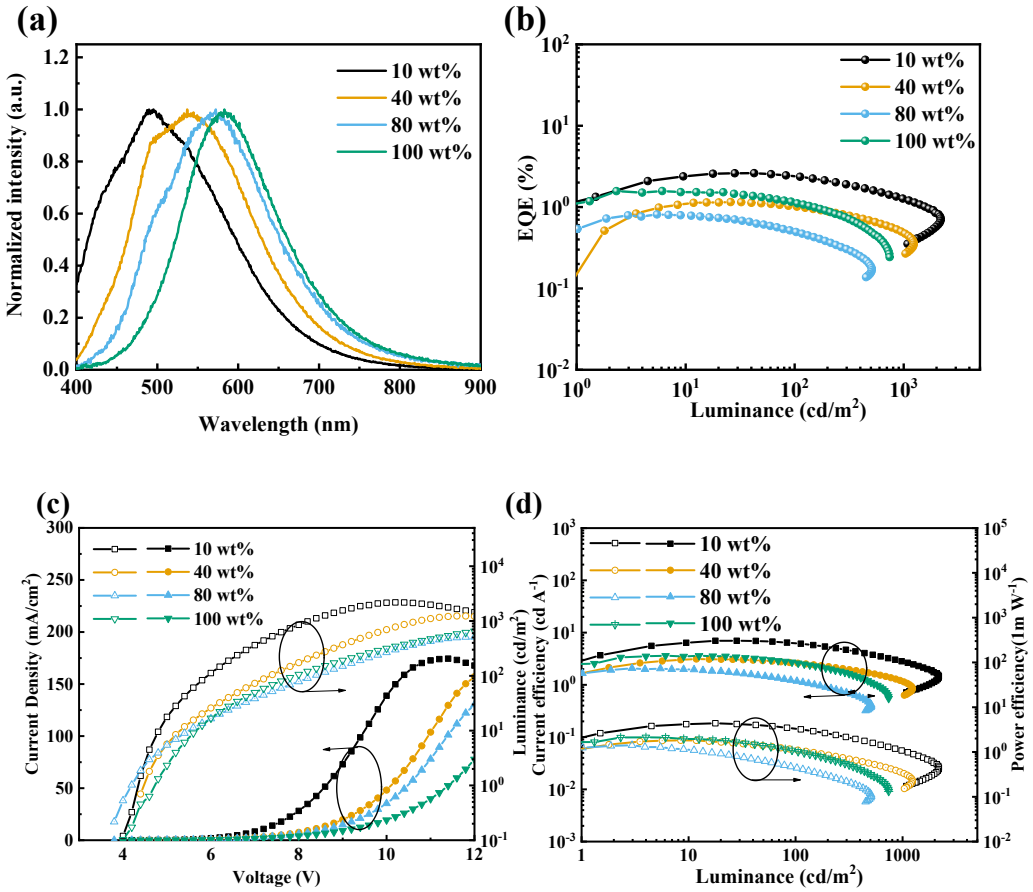

Figure S15. Performance of **BP2**-based OLED with doped different concentration (10%, 40%, 80%, and 100%. (a) EL spectra at 12V. (b) External quantum efficiency (η_{ext}) versus current density plots. (c) Current density and luminance versus voltage (*J-V-L*) characteristics. (d) Current efficiency-luminance-power efficiency.

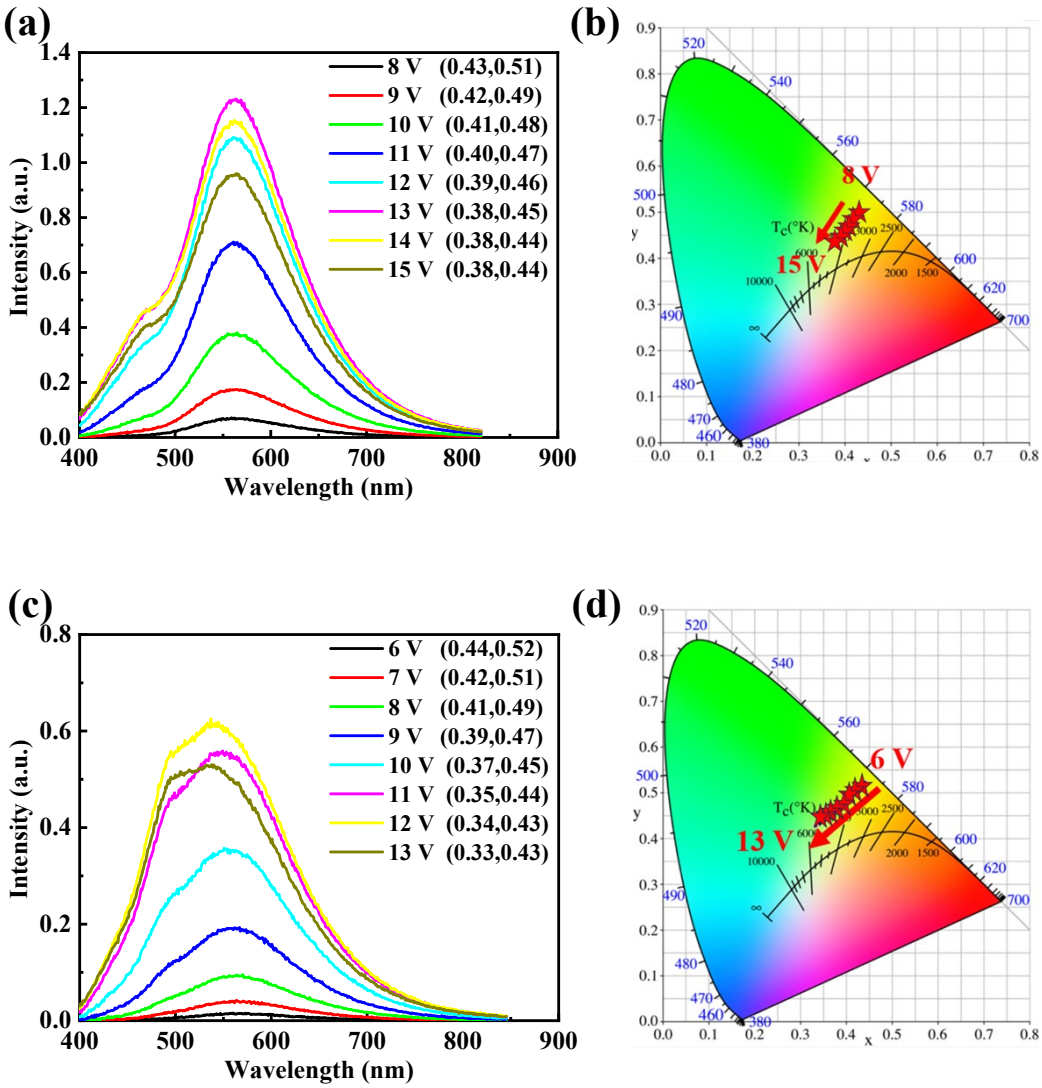

Figure S16. (a) EL spectra of devices based on 10 wt. % **BP1**: CBP at different voltages. (b) CIE 1931 coordinates of 10 wt. % **BP1**: CBP devices; (c) EL spectra of 40 wt. % **BP2**: CBP based devices at different voltages; (d) CIE 1931 coordinates of 40 wt. % **BP2**: CBP devices.

Table S1. The PLQYs of **BP1** and **BP2**.

Emitters	**BP1**	**BP2**
PLQYs	4.53%[a] /17.02%[b]	3.49%[a] /19.68%[b]

[a] Toluene; [b]10 wt. % (**BP1**/ **BP2**): CBP film.

Table S2. The calculates potential energy for the "ax" and "eq" conformations in vacuum.[2]

Compd	Potential Energy (Hartree)			Energy Difference		Activation Energy for "ax"		Activation Energy for "eq"	
	"ax"	"eq"	Barrier	(Hartree)	(eV)	(Hartree)	(eV)	(Hartree)	(eV)
BP1	–2140.32148	–2140.31742	–2140.31474	–0.00406	0.1105	–0.00674	0.1834	–0.00268	0.0729
BP2	–2140.31850	–2140.31310	–2140.31057	–0.00540	0.1469	–0.00793	0.2158	–0.00253	0.0688

Table S3. Summary of OLED performances using **BP1**.

concentration	V_{on} (V)[a]	L_{max} (cd m^{-2}) [b]	CE_{max} (cd A^{-1}) [c]	PE_{max} (1m W^{-1}) [d]	EQE_{max} (%)[e]	λ_{EL} (nm)[f]	CIE (X, Y)[g]
non-doped	4.6	773	1.596	0.794	0.79	588	(0.50, 0.47)
80 wt%	4.6	849	1.915	0.845	0.86	585	(0.49, 0.48)
40 wt%	4.4	2715	2.548	0.980	1.02	573	(0.45, 0.49)
10 wt%	5.0	2264	7.612	3.334	2.92	561, 466	(0.38, 0.44)

[a] Start-up voltage; [b] Maximum brightness; [c] Maximum current efficiency; [d] Maximum power efficiency; [e] Maximum external quantum efficiency; [f] Wavelength with voltage of 14 V; [g] Color 1931 coordinates.

Table S4. Summary of OLED performances using **BP2**.

concentration	V_{on} (V)[a]	L_{max} (cd m^{-2}) [b]	CE_{max} (cd A^{-1}) [c]	PE_{max} (1m W^{-1}) [d]	EQE_{max} (%)[e]	λ_{EL} (nm)[f]	CIE (X, Y)[g]
non-doped	4.0	742	3.605	2.130	1.57	583	(0.46, 0.48)
80 wt%	3.8	510	2.074	1.297	0.81	567	(0.41, 0.47)
40 wt%	4.2	1236	3.113	1.820	1.15	536	(0.34, 0.43)
10 wt%	3.4	2186	6.976	4.378	2.61	493	(0.33, 0.36)

[a] Turn-on voltage; [b] Maximum luminance; [c] Maximum current efficiency; [d] Maximum power efficiency; [e] Maximum external quantum efficiency; [f] Wavelength with a voltage of 12 V; [g] Color 1931 coordinates.

NMR Spectra and HRMS

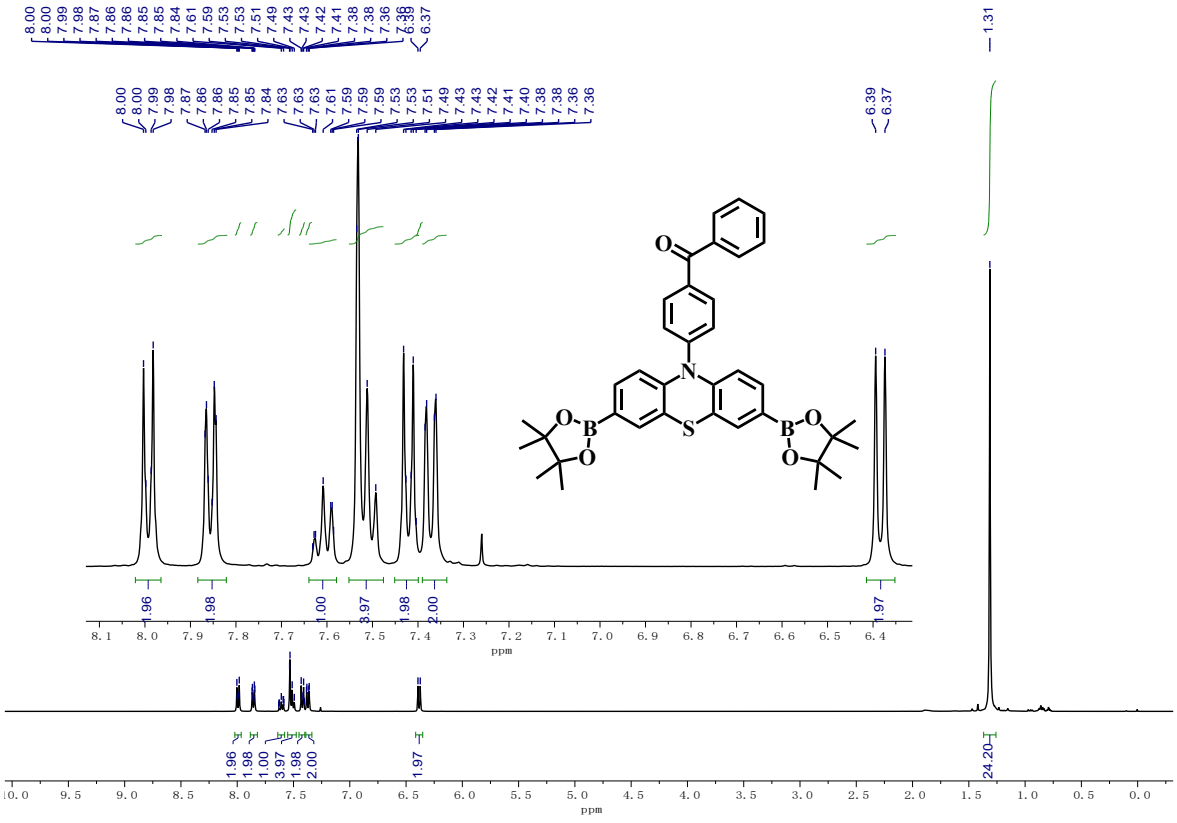

^{1}H NMR (400 MHz, $CDCl_3$) of compound **3**.

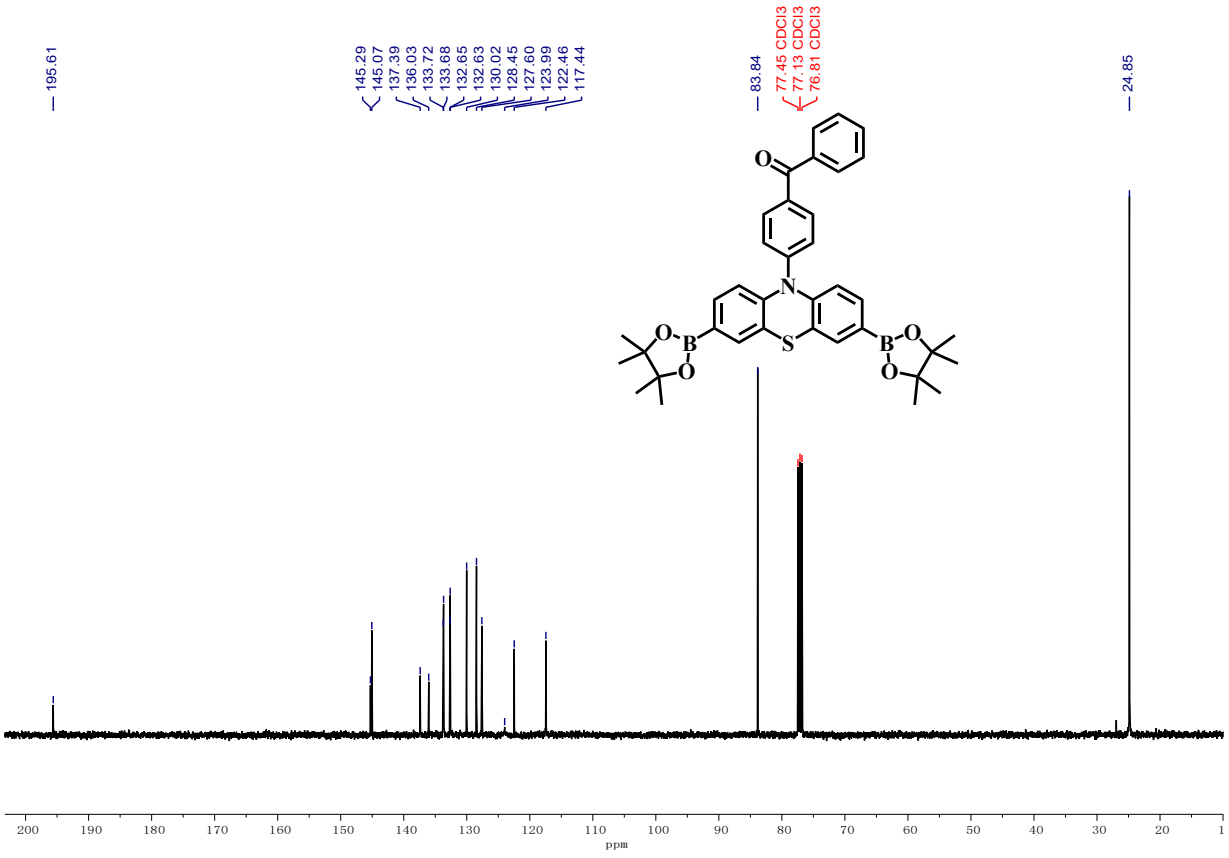

^{13}C NMR (100 MHz, $CDCl_3$) of compound **3**.

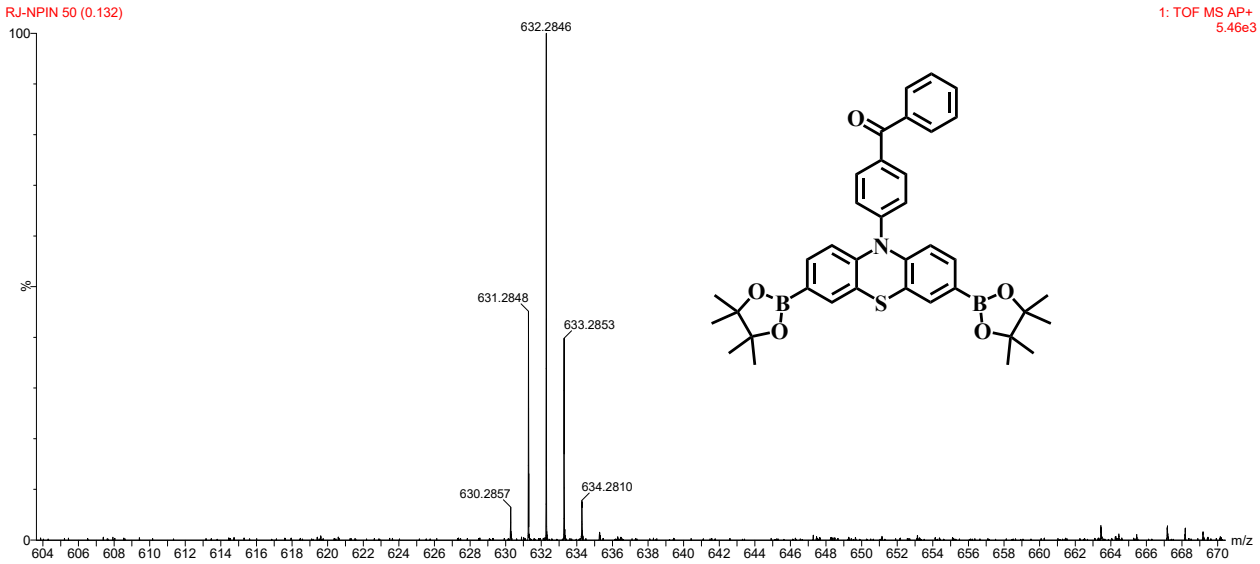

HRMS (MALDI–TOF) of compound **3**.

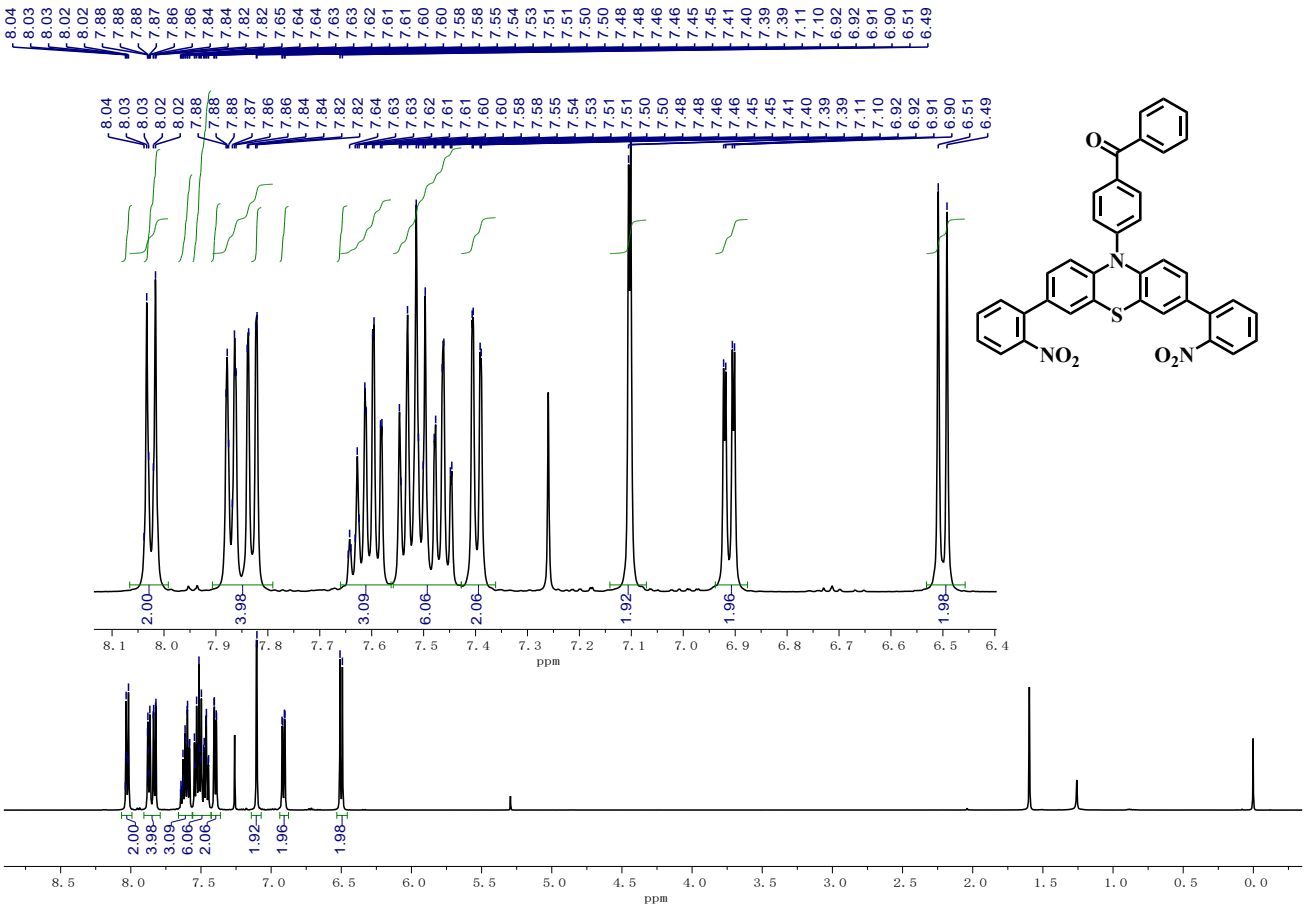

^{1}H NMR (500 MHz, $CDCl_3$) of compound **4**.

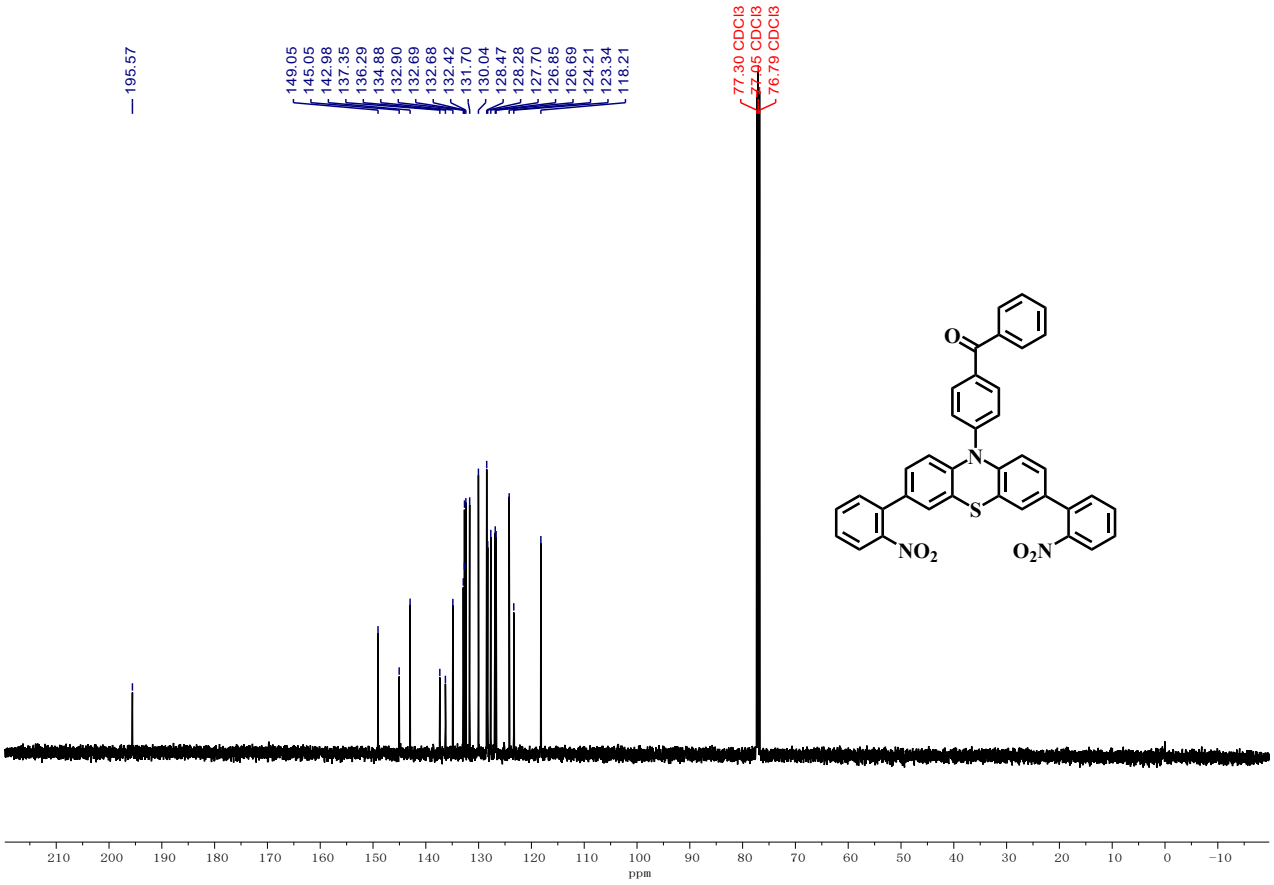

^{13}C NMR (125 MHz, $CDCl_3$) of compound **4**.

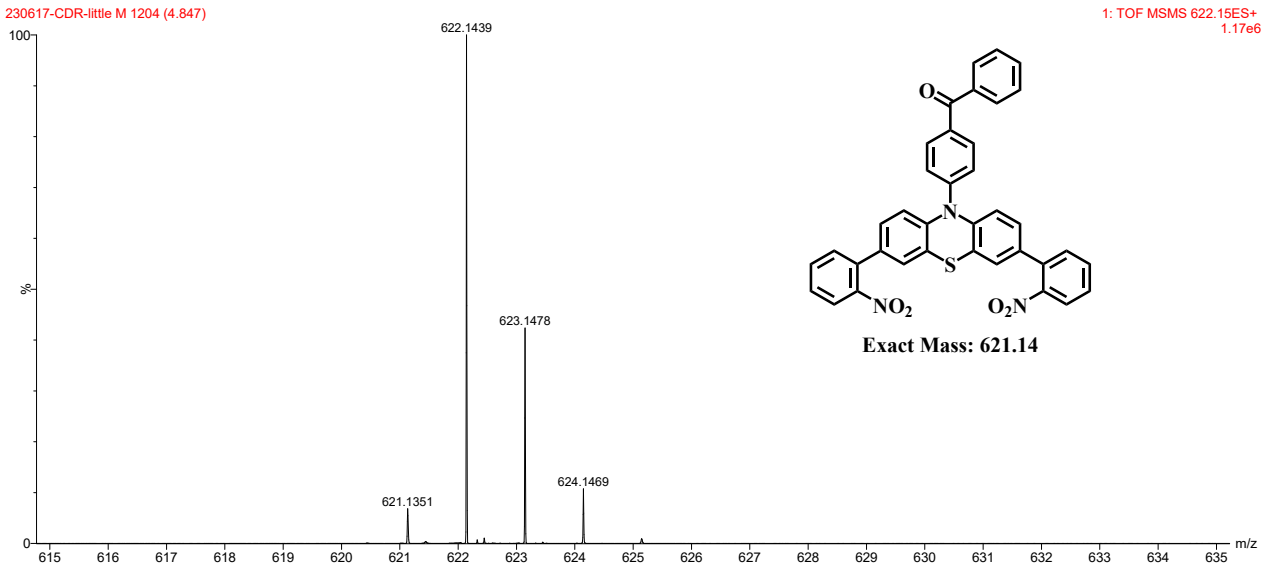

HRMS (MALDI–TOF) of compound **4**.

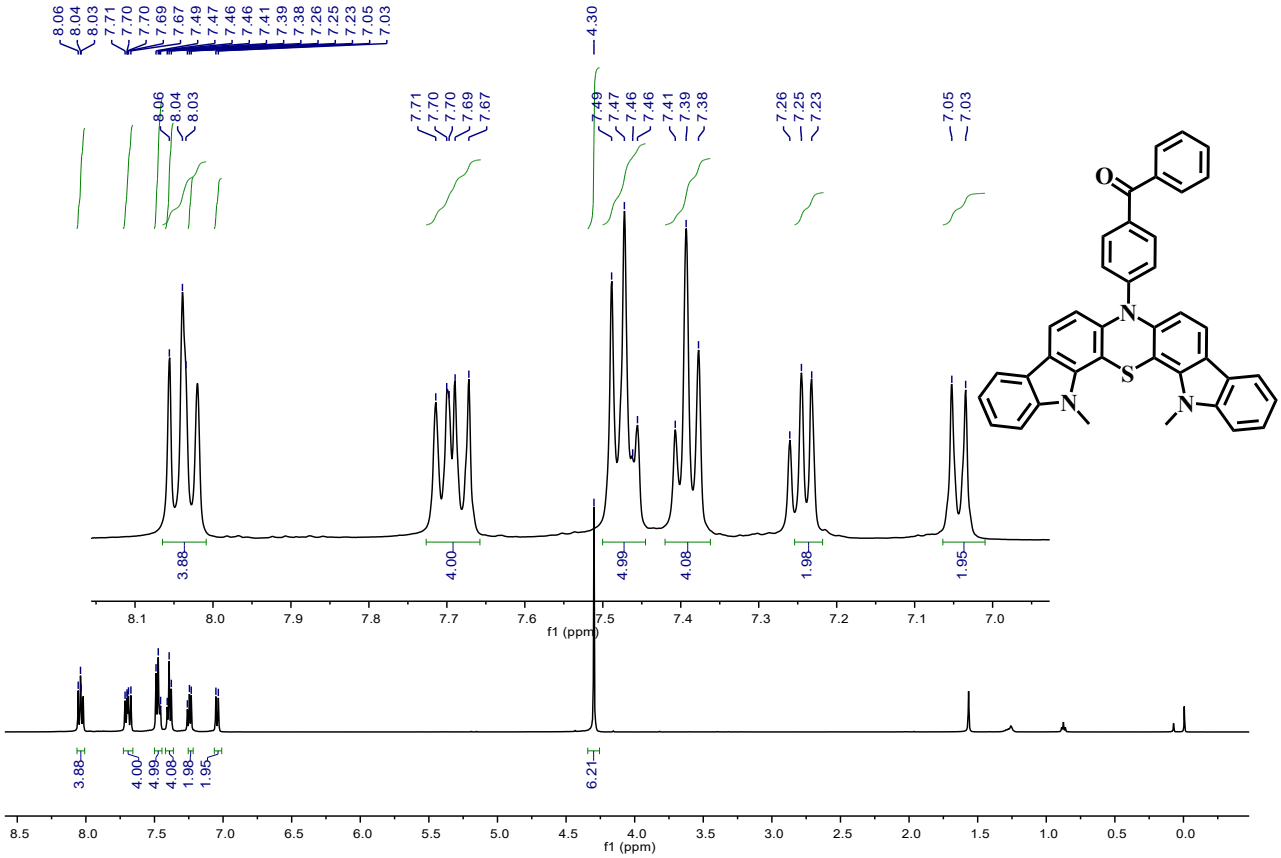

^{1}H NMR (500 MHz, $CDCl_3$) of **BP2**.

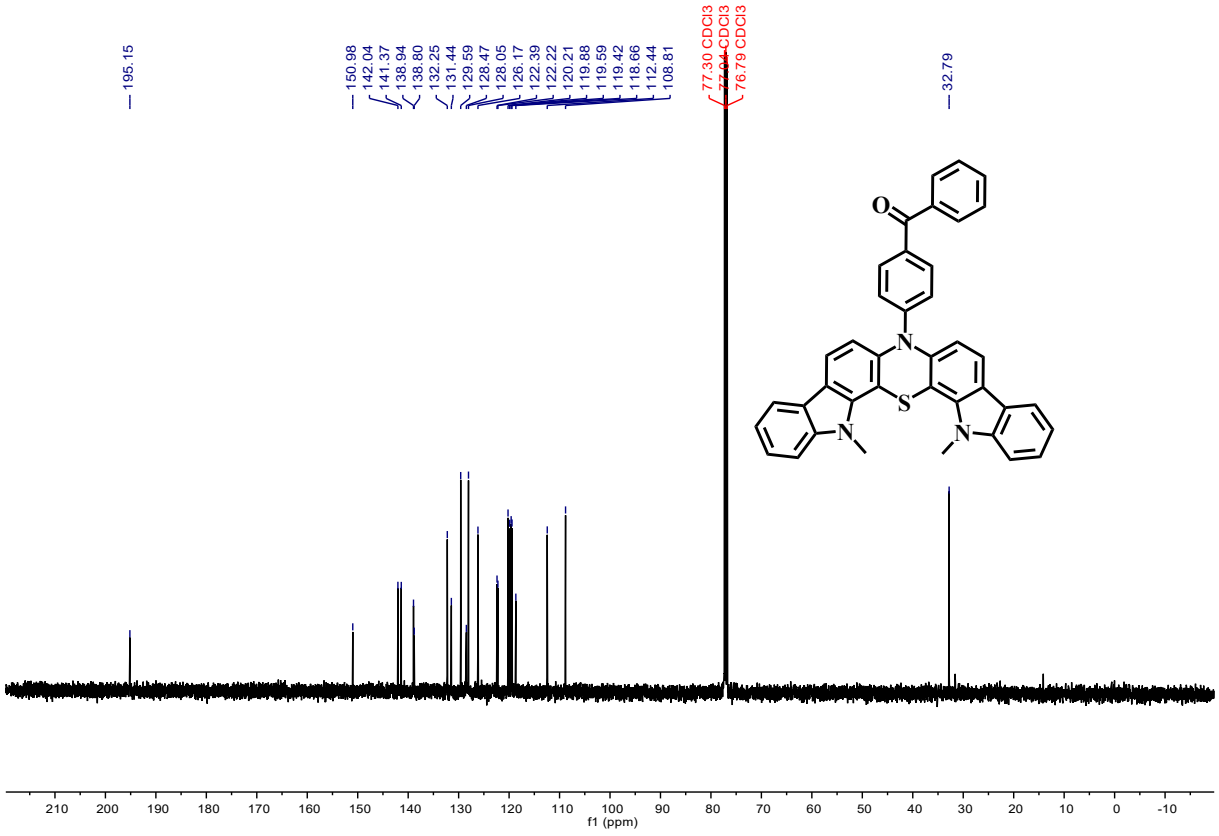

^{13}C NMR (125 MHz, $CDCl_3$) of **BP2**.

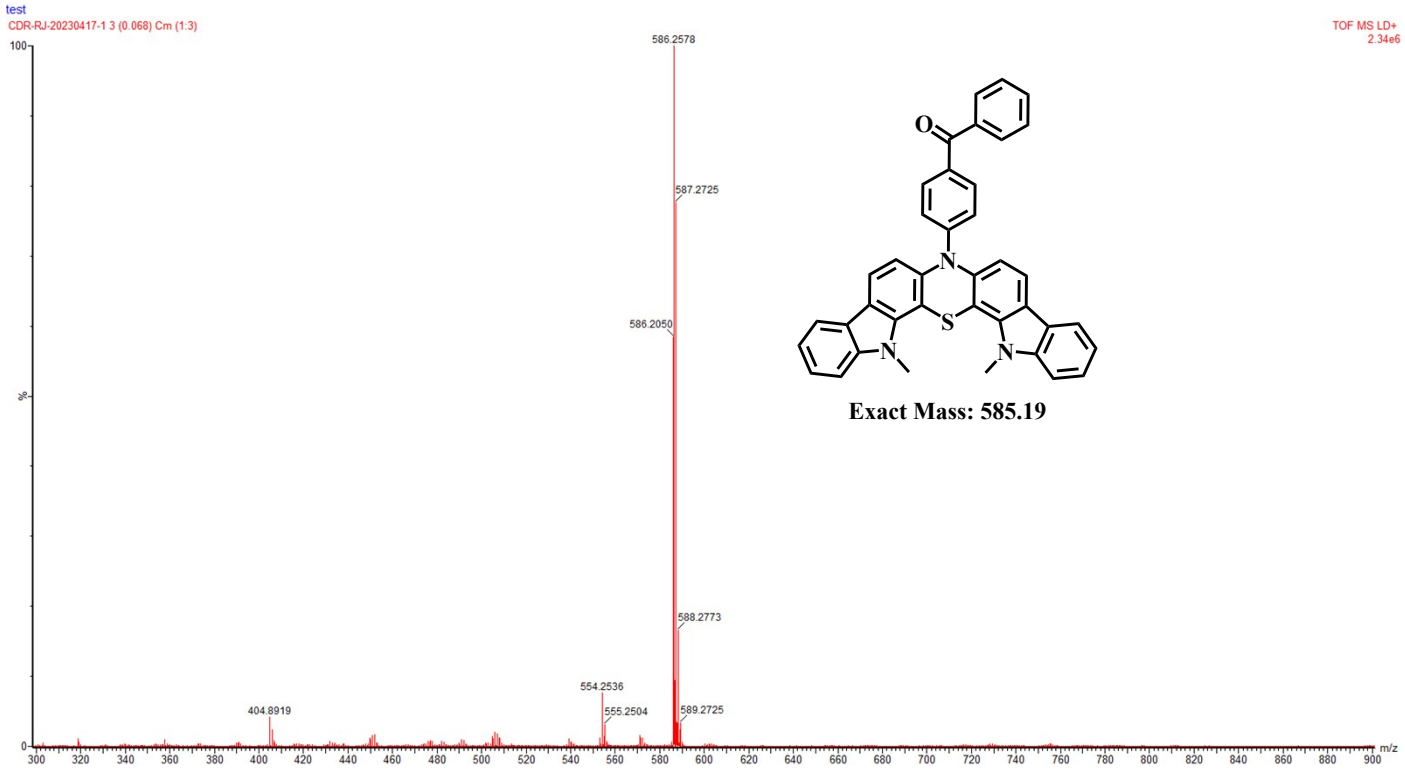

HRMS (MALDI–TOF) of **BP2**.

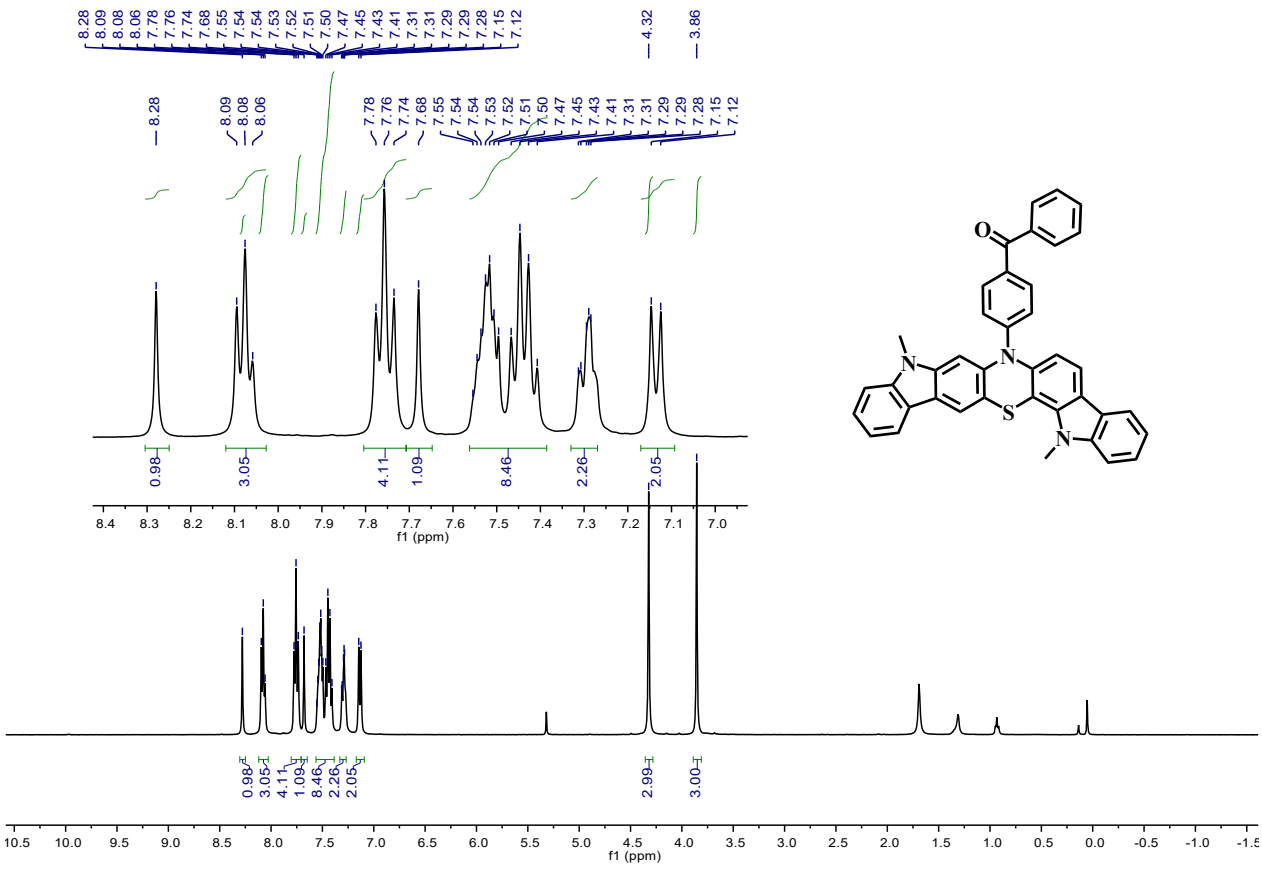

^{1}H NMR (400 MHz, $CDCl_3$) of **BP1**.

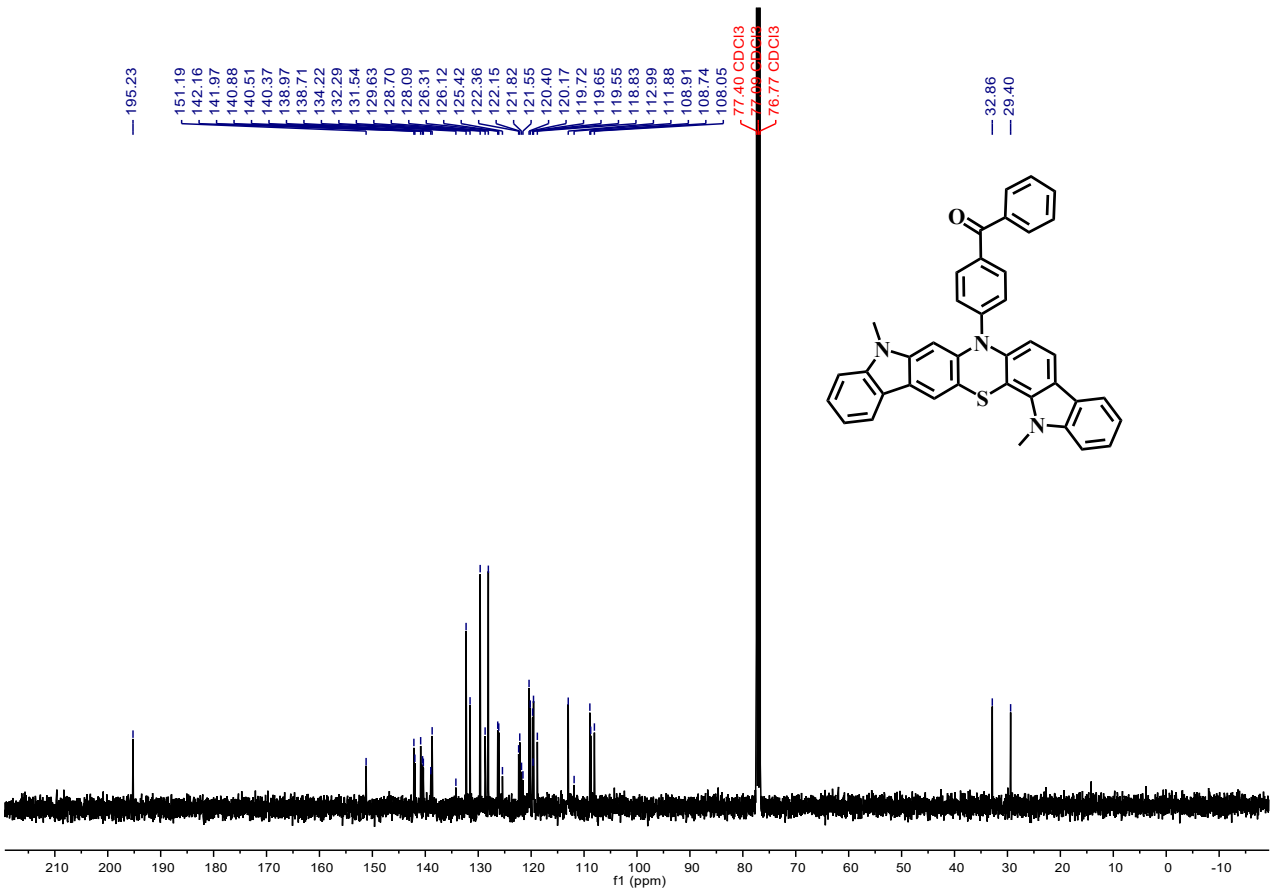

^{13}C NMR (100 MHz, $CDCl_3$) of **BP1**.

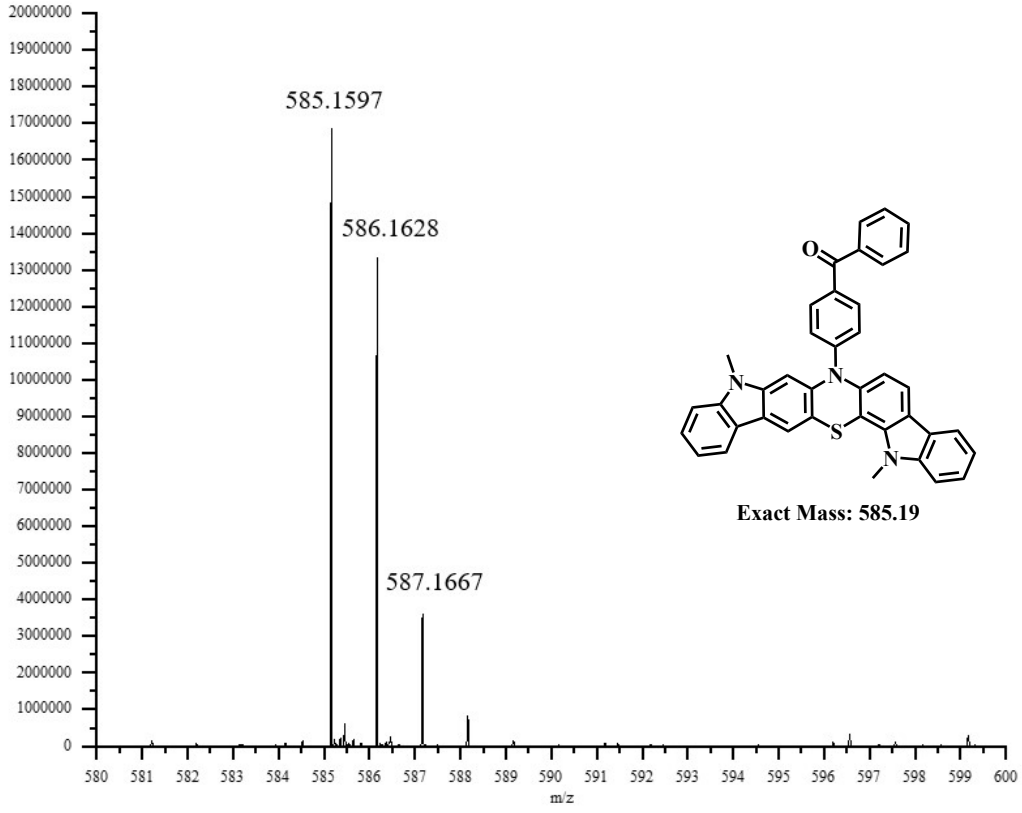

HRMS (MALDI–TOF) of **BP1**.

3. Reference

1. W. Qiu, X. Cai, M. Li, L. Wang, Y. He, W. Xie, Z. Chen, M. Liu and S.-J. Su, *Journal of Materials Chemistry C*, 2021, **9**, 1378-1386.
2. K. Wang, C.-J. Zheng, W. Liu, K. Liang, Y.-Z. Shi, S.-L. Tao, C.-S. Lee, X.-M. Ou and X.-H. Zhang, *Advanced Materials*, 2017, **29**, 1701476.